Materials **2013**, *6*, 4654-4674; doi:10.3390/ma6104654

OPEN ACCESS

materials

ISSN 1996-1944

www.mdpi.com/journal/materials

Review

Thermodynamic Tuning of Mg-Based Hydrogen Storage Alloys: A Review

Min Zhu [1,2,*], Yanshan Lu [1,2], Liuzhang Ouyang [1,2] and Hui Wang [1,2]

[1] School of Materials Science and Engineering, South China University of Technology, Guangzhou 510641, China; E-Mails: yanshan.lu@mail.scut.edu.cn (Y.L.); meouyang@scut.edu.cn (L.O.); mehwang@scut.edu.cn (H.W.)

[2] Key Laboratory of Advanced Energy Storage Materials of Guangdong Province, Guangzhou 510641, China

* Author to whom correspondence should be addressed; E-Mail: memzhu@scut.edu.cn; Tel.: +86-20-8711-3924; Fax: +86-20-8711-1317.

Received: 28 August 2013; in revised form: 26 September 2013 / Accepted: 12 October 2013 / Published: 18 October 2013

Abstract: Mg-based hydrides are one of the most promising hydrogen storage materials because of their relatively high storage capacity, abundance, and low cost. However, slow kinetics and stable thermodynamics hinder their practical application. In contrast to the substantial progress in the enhancement of the hydrogenation/dehydrogenation kinetics, thermodynamic tuning is still a great challenge for Mg-based alloys. At present, the main strategies to alter the thermodynamics of Mg/MgH_2 are alloying, nanostructuring, and changing the reaction pathway. Using these approaches, thermodynamic tuning has been achieved to some extent, but it is still far from that required for practical application. In this article, we summarize the advantages and disadvantages of these strategies. Based on the current progress, finding reversible systems with high hydrogen capacity and effectively tailored reaction enthalpy offers a promising route for tuning the thermodynamics of Mg-based hydrogen storage alloys.

Keywords: Mg-based hydrogen storage alloys; thermodynamics; alloying; nanostructuring; changing reaction pathway

1. Introduction

Modern civilization would not be sustainable without sufficient energy and a clean environment. However, severe challenges will arise from the shortage of fossil energy resources (coal, oil, and natural gas) and environmental pollution, owing to massive and long-term use of fossil fuels. Thus, it is very important to develop clean and renewable energy sources to replace fossil fuels.

Hydrogen is considered to be one of the most promising energy carriers for the future, because it is abundant, has high energy density (142 MJ/kg, three times higher than that of gasoline), and its combustion product is environmentally benign water [1]. However, hydrogen exists as a gas under atmospheric conditions and is highly flammable, explosive, and diffusible. Thus, storing hydrogen in a safe and efficient way is very important, but difficult, for hydrogen to be used as an energy source.

Hydrogen storage methods can be classified into three types: high-pressure gas storage, low-temperature liquid storage, and solid-state storage. Although compressed hydrogen gas technology is relatively mature, the energy content per unit volume is only 4.4 MJ/L at pressures as high as 70 MPa, which is much less than that of gasoline (31.6 MJ/L) [2]. In addition, it has other drawbacks such as risks due to the very high pressures and large energy consumption during compression. Liquid hydrogen storage (8.4 MJ/L) has almost twice the energy content of hydrogen gas [2]. However, hydrogen liquefaction requires cooling to −252 °C, which is expensive and there are problems with inevitable evaporative loss [2,3]. Solid-state hydrogen storage involves storing hydrogen in solid-state materials through physical or chemical absorption, and is considered as the most promising method owing to its high energy density and safety. Currently, solid-state materials such as carbon materials, zeolites, and metal organic frameworks (MOFs) adsorb molecular hydrogen mainly through physisorption, while metal hydrides, complex hydrides, and chemical hydrides (e.g., ammonia borane) store atomic or ionic hydrogen by chemical bonding.

Figure 1 shows the volumetric *versus* gravimetric hydrogen density of the various hydrogen storage methods [4]. Taking into account storage density, energy consumption, and safety, metal hydrides and complex hydrides are the most promising materials for solid-state hydrogen storage. Metal hydrides usually consist of an element A (e.g., Ti, Zr, Mg, and Re) and an element B (e.g., Fe, Co, Ni, and Cu) that tend to form a stable and an unstable hydride, respectively. Based on the atomic ratio of A to B, metal hydrides can be classified as AB_5, AB_3, AB_2, AB type compounds.

$LaNi_5$ has a $CaCu_5$ type structure and is a typical example of an AB_5 type alloy [5]. At ambient temperature, $LaNi_5H_6$ forms upon hydrogenation with a theoretical hydrogen capacity of about 1.4 wt % and a formation enthalpy of −30.2 kJ/mol. A successful application of the AB_5 type alloys has been achieved using the negative electrode in Ni/MH batteries. Substitution of La in $LaNi_5$ with Mm (mischmetal) and Ni with Mn, Co, and Al is beneficial for improving the cycle-life and reducing the cost. One of the AB_5 type alloys with excellent properties is $MmNi_{3.55}Al_{0.4}Mn_{0.3}Co_{0.75}$ [6]. The AB_2 and AB type alloys, which have Laves and B2 structures, and hydrogen storage capacities of about 2.0 wt % and 1.8 wt %, respectively. These alloys have also been used in practical applications such as rechargeable batteries, hydrogen sources for fuel, and hybrid compressed hydrogen cylinders [7,8].

To increase the hydrogen storage capacity, Mg is added into the AB_5 alloys, and AB_3 type ($PuNi_3$ or $CeNi_3$ structure) alloys are obtained. The AB_3 structure contains a long-range stacking arrangement of which one-third is AB_5-like and two-thirds is AB_2-like. Chen *et al.* [9] prepared $LaNi_3$ and $CaNi_3$ using

a powder metallurgy method. Composition optimization is very important for achieving excellent electrochemical performance, including capacity, rate capability, and cycle-life. Kohno *et al.* [10] reported that partially substituting Ni by Al, Fe, Mn, Si, Sn, and Cu increases the discharge capacity of $La(Ni_{0.9}M_{0.1})_3$ alloy electrodes at room temperature. By partial substitution, AB_3 alloys, such as $LaCaMgNi_9$, $CaTiMgNi_9$, $LaCaMgNi_6Al_3$, and $LaCaMgNi_6Mn_3$, were also synthesized. All of these alloys can be easily activated at room temperature under a hydrogen pressure of 3.3 MPa and can absorb/desorb 1.8 wt % hydrogen [9]. The theoretical discharge capacity of the AB_3 alloy electrode $LaCaMgNi_9$ is 484 mAh/g, which is 30% higher than that of the AB_5 alloys (372 mAh/g) [11]. Peng *et al.* [12] developed a $Ml_{0.7}Mg_{0.3}Ni_{3.2}$ (Ml denotes La-rich mischmetal) hydrogen storage alloy by induction melting and found that the alloy had a multi-phase microstructure containing $(MlMg)Ni_3$, $(MlMg)Ni_2$, and $MlNi_5$ phases with a maximum hydrogen storage capacity of 1.7 wt % at room temperature. They also found that the grain size has a large effect on the hydrogen storage capacity of AB_3-base Ml–Mg–Ni multi-phase alloys. The hydrogen storage capacity decreases with decreasing grain size, which is due to poor hydrogen storage in the grain boundary region [13].

Figure 1. Volumetric and gravimetric hydrogen density of some hydrides (Reprinted with permission from [4], Copyright 2003 Elsevier).

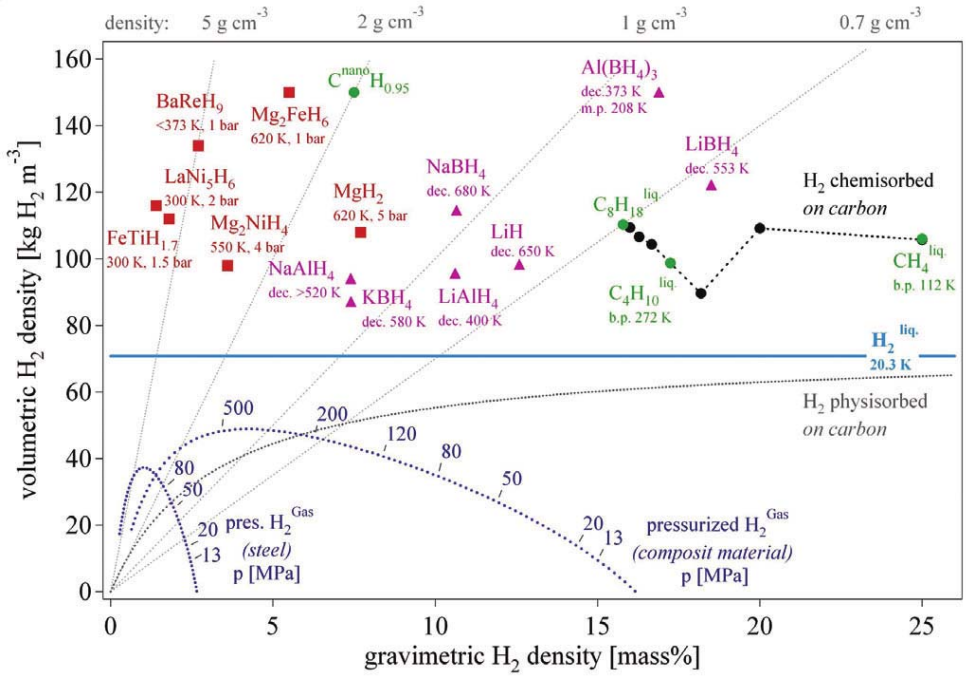

The above mentioned metal hydrides have suitable hydrogen sorption thermodynamics and fast kinetics, which means that hydrogen sorption can take place with a fast rate at suitable temperatures and hydrogen pressure conditions. However, they all have low gravimetric hydrogen storage density and do not satisfy the application requirements as energy sources, in particular the goal for the storage of at least 5.5 wt % by the year 2017 set for onboard automotive hydrogen storage systems by the United States Department of Energy (DOE) [14]. Mg-based hydrides have relatively high storage capacity (theoretically 7.6 wt % for MgH_2), are abundant and inexpensive, and are considered to be the most promising metallic hydrogen storage materials. However, poor kinetics and high operating temperatures (up to about 300 °C at 1 atm hydrogen pressure) hinder their practical application. Thus,

tuning the kinetics and thermodynamics of Mg-based hydrides is the key issue to overcome the problems limiting their practical application. Significant progress has been made in improving the hydrogenation/dehydrogenation kinetics of Mg-based alloys, which will be briefly reviewed in the following sections. However, tuning of the thermodynamic properties is still a great challenge, and we will review the progress in detail.

2. Thermodynamic and Kinetic Characteristics of Mg-Based Hydrogen Storage Alloys

Pure Mg has a hexagonal crystal structure, and it can react reversibly with hydrogen to form MgH_2. As the hydrogen pressure increases, the crystal structure of MgH_2 changes to tetragonal β-MgH_2. At ambient temperature and high hydrogen pressure (GPa), β-MgH_2 transforms to orthorhombic γ-MgH_2. γ-MgH_2 is a metastable phase and decomposes to the stable β-MgH_2 phase at temperatures above 350 °C. Table 1 shows the crystal structure data of Mg, β-MgH_2, and γ-MgH_2.

Table 1. Crystallographic data of Mg, β-MgH_2, and γ-MgH_2.

Phase	Space group	Lattice parameters (Å)	Prototype
Mg	$P6_3/mmc$	a = 3.2094, c = 5.2112 (PDF#35-0821)	Mg
β-MgH_2	$P4_2/mnm$	a = 4.5170, c = 3.0205 (PDF#12-0697)	Rutile TiO_2
γ-MgH_2	*Pbcn*	a = 4.5300, b = 5.4400, c = 4.9300 (PDF#35-1184)	α-PbO_2

Because of the strong ionic characteristics of the Mg–H bond, the desorption temperature of MgH_2 is relatively high. The enthalpy can be used to characterize the strength of metal-H bonds, and the enthalpy and entropy can be calculated by the van't Hoff equation according to the equilibrium hydrogen pressure and the corresponding temperature in the pressure-composition isotherm (PCI) of hydrogen absorption/desorption. The measured thermodynamic data of MgH_2 from different works are shown in Table 2. The desorption enthalpy of MgH_2 is much larger than practical requirements for metal hydrides of 20–40 kJ/mol. Corresponding to its thermodynamic characteristics, the equilibrium hydrogen desorption temperature is 289 °C under 1 atm hydrogen pressure. Thus, from a thermodynamic point of view, Mg/MgH_2 is unsuitable for practical application as a hydrogen storage material unless the ΔH of Mg-based alloys can be decreased. ΔS is another important thermodynamic value for hydrogen desorption. The entropy has been considered to be a constant value of about 130 J/(mol·K), however, recent studies have shown that ΔS of the desorption process is variable [15,16]. Therefore, increasing the entropy would be a useful way of lowering the operating temperature if ΔH did not significantly change.

Table 2. ΔH and ΔS for MgH_2 decomposition in different works.

Different works	ΔH (kJ/mol)	ΔS [J/(mol·K)]
Stampfer [17]	74.4 ± 0.3	135.1 ± 1.9
Reilly [18]	77.4 ± 4.2	138.3 ± 2.9
Pedersen [19]	70	126
Friedlmeier [20]	74.3 ± 0.5	136 ± 1
Shao [21]	75.0	135.6
Bardhan [22]	75	130

Apart from the above mentioned thermodynamic restrictions, the poor kinetics of Mg-based hydrides also result in its high operating temperature and limit its practical use. Figure 2 shows the hydrogenation kinetic curves of conventional Mg powder. The hydrogen absorption capacity was almost negligible when heated up to 300 °C. Even when the powder was heated to 400 °C, the hydrogen absorption capacity was less than 2 wt % after 2 h [23]. For the dehydrogenation of unmilled MgH2 (Figure 3), there is no obvious desorption at 573 K within 2000 s. Even at 623 K, it takes more than 3000 s to completely desorb. The high activation energy (ΔE) for hydrogen desorption from unmilled MgH_2 (about 156 kJ/mol) is a clear indication of the poor kinetics [24].

Figure 2. Hydrogen absorption by a conventional, non-catalyzed magnesium powder (Reprinted with permission from [23]. Copyright 1999 Elsevier).

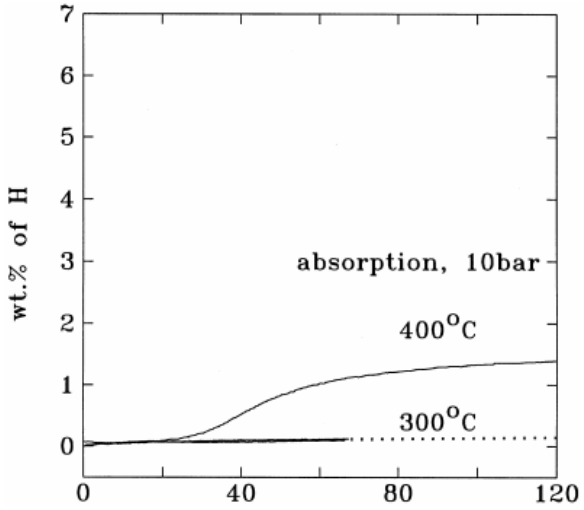

Figure 3. Hydrogen desorption curves of unmilled (solid symbols) and ball-milled (hollow symbols) MgH_2 under a hydrogen pressure of 0.015 MPa (Reprinted with permission from [24]. Copyright 1999 Elsevier).

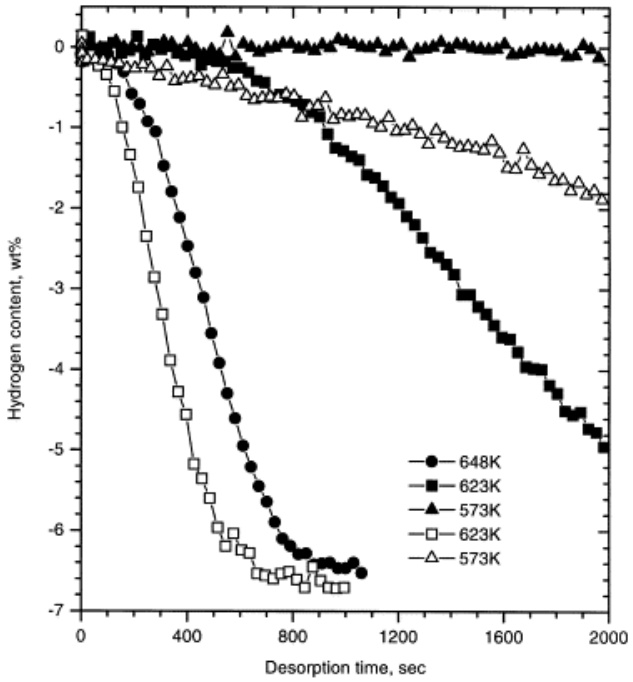

There are several reasons for the sluggish hydrogenation kinetics: (1) a layer of MgO or $Mg(OH)_2$ can easily form on the surface and inhibit the dissociation of molecular H_2 on the surface and diffusion of atomic H into the bulk; and (2) the diffusion of H is extremely difficult after a MgH_2 layer forms on the surface of Mg because the H_2 diffusion coefficient in MgH_2 (1.5×10^{-16} m^2/s) is considerably smaller than that in Mg (4×10^{-13} m^2/s) [25]. The main reasons for the sluggish dehydrogenation kinetics are: (1) the difficulty of breaking the Mg–H bond; (2) the low diffusion rate of H in MgH_2; (3) the high energy required for the nucleation of Mg on the surface of MgH_2; and (4) recombination of hydrogen atoms to form the hydrogen molecule on the Mg surface [26–28].

3. Progress in Improving the Hydrogen Absorption/Desorption Kinetics of Mg-Based Alloys

To accelerate the hydrogen absorption/desorption kinetics of Mg-based hydrides, tremendous efforts have been devoted to develop methods of catalyzing, nanostructuring, and forming Mg-based composites. Significant progress has been achieved through those efforts.

Transition metals and metal oxides have proved to be effective catalysts for hydrogen absorption/desorption of Mg-based hydrides. Liang *et al.* [29] mixed MgH_2 with the 3d elements Ti, V, Mn, Fe, and Ni by mechanical milling. All of the additives drastically decreased the activation energy of hydrogen desorption of MgH_2. The MgH_2–V composite showed the most rapid desorption kinetics, and its activation energy of 62.3 kJ/mol is much smaller than that of ball-milled pure MgH_2 (120 kJ/mol [24]), while the composite containing Ti exhibited the most rapid absorption kinetics. Bormann *et al.* [30] produced nanocrystalline MgH_2/Me_xO_y (Me_xO_y = Sc_2O_3, TiO_2, V_2O_5, Cr_2O_3, Mn_2O_3, Fe_3O_4, CuO, Al_2O_3, and SiO_2) powders via high-energy ball milling. Compared with the pure nanocrystalline materials, some oxides lead to an enormous catalytic acceleration of hydrogen sorption. Cr_2O_3 gave the fastest hydrogen absorption, and the composite material containing Fe_3O_4 showed the fastest desorption kinetics. Later, they found that the catalytic effect of Nb_2O_5 was superior for the hydrogen sorption reaction of magnesium compared with other metal and oxide catalysts, with absorption and desorption of 7 wt % hydrogen possible within 60 s and 130 s at 300 °C, respectively [31]. The additives catalyze the reaction by promoting the recombination of hydrogen atoms to form the hydrogen molecule. The catalytic activity of the additives is influenced by four distinct physico-thermodynamic properties: a high number of structural defects, a low stability of the compound, a high valence state of the transition-metal ion within the compound, and a high affinity of the transition-metal ion for hydrogen [32]. However, the thermodynamics of MgH_2 are obviously not changed by adding the catalysts.

Nanostructuring is an efficient way of improving the kinetics of Mg-based alloys. Ball milling is a common method to prepare nanocrystalline Mg-based hydrides, and significantly increases the hydrogen uptake/release rates of Mg/MgH_2 because it destroys the oxide layers on the surface of Mg, introduces a large number of defects, and decreases the diffusion lengths of H. Ball-milled MgH_2 completely desorbed at 350 °C after 700 s, and reabsorbed in 750 s at 300 °C [24]. To overcome the drawback of the high oxidation sensitivity of Mg-based materials, especially at the nanoscale in air, Jeon *et al.* [33] prepared an air-stable composite material consisting of metallic Mg nanocrystals (NCs) in a gas-barrier polymer matrix that was capable of both storing a high density of hydrogen (up to

6 wt % of Mg, 4 wt % for the composite) and rapid kinetics (loading in <30 min at 200 °C). Moreover, nanostructuring of Mg results in rapid storage kinetics without using expensive heavy-metal catalysts.

In situ formation of a nanocomposite, in which catalyst phases are involved, is another efficient way of improving the kinetics of Mg-based alloys. Ouyang *et al.* prepared a series of Mg_3RE (RE = La [34], Pr [35], Nd [36], and mischmetals [37]) alloys by induction melting. All of the alloys could absorb hydrogen at room temperature with rapid hydrogenation/dehydrogenation kinetics. After the first hydrogenation, MgH_2 and REH_x composites were formed, although REH_x was almost unchanged in the subsequent hydrogenation/dehydrogenation cycles. The nanometer-sized REH_x formed *in situ* during the activation process showed good catalytic properties for increasing the kinetics. The kinetics could be further accelerated by alloying Mg_3RE with transition metals such as Ni and Co [34,35,38]. Recently, Liu *et al.* [39] prepared the $Mg_{91.9}Ni_{4.3}Y_{3.8}$ alloy composed of a large amount of long-period stacking ordered (LPSO) phases. The alloy showed excellent dehydrogenation kinetics and could release about 5 wt % hydrogen at 300 °C within 200 s. At the first hydrogenation reaction, the LPSO phases transformed into MgH_2, Mg_2NiH_x, and YH_x. Although the transformations could not reversibly take place during the subsequent hydrogenation reaction, the highly dispersed and nanostructured composite (MgH_2 + Mg_2NiH_x and YH_x) remained after the hydrogenation/dehydrogenation cycles, which effectively promotes the dehydrogenation performance of the alloy. In addition, YH_x and Mg_2NiH_x can also act as a catalyst for the hydrogenation/dehydrogenation of the alloy.

The hydrogen storage properties of Mg-based alloys have also been improved by *in situ* formation of nanocomposites with the melt-spun method. Under condition of rapid solidification, Mg–Ni–RE (RE = rare earth metal or Y) alloys can be easily amorphized. Spassov et al. [40,41] prepared a series of nanocrystalline and nano-amorphous Mg–Ni–RE alloys with good hydrogen storage properties by rapid quenching. For example, the as-quenched $Mg_{75}Ni_{20}Mm_5$ alloy could absorb 4.0 wt % H_2 at 25 °C in 100 min. The $Mg_{75}Ni_{20}Mm_5$ alloy consisted of nanocrystals embedded in an amorphous phase, and the amorphous phase around the nanocrystals gave hydrogen easier access to the nanograins, avoiding the long-range diffusion of hydrogen through an already formed hydride, which is often the slowest step of absorption. Lin *et al.* [42] reported that after only one activation cycle under H_2 (4 MPa) at 300 °C, melt-spun $Mg_3LaNi_{0.1}$ alloy could absorb 2.7 wt % hydrogen at room temperature within 3 min, and the minimum hydrogen desorption temperature was 224 °C, which is 33 °C lower than that of the $Mg_3LaNi_{0.1}$ melt. This improvement was attributed to the catalytic role of the *in situ* formed nanocrystalline Mg_2Ni and LaH_2.

Forming Mg-based composites with other hydrogen storage alloys can enhance the hydriding process of Mg, which is due to the key role played by the interphase boundary in the interaction between the different components of the composite. Zhu *et al.* [43] prepared Mg-MmM_5 ($LaNi_5$-based RE alloys) nano-phase composite hydrogen storage alloys by mechanical alloying. Figure 4a shows that in the MmM_5–10% Mg and MmM_5–30% Mg systems, nanocrystalline Mg can quickly absorb hydrogen at room temperature. The hydrogen absorption kinetic curves were fitted using various rate equations to reveal the mechanism of the hydriding reaction process. For the nano-phase composite, the hydriding reaction was in agreement with the rate equation $\ln[\alpha/(1-\alpha)] = k(t - t_c)$ of an auto-catalysis process. Figure 4b is a secondary electron image of MmM_5–10% Mg powder obtained by milling for 20 h. After the long milling time, the brittle MmM_5 component was very fine and bonded to softer Mg, forming composite particles that contain a very high density of interfaces [44].

Gross *et al.* [45] produced La_2Mg_{17}–$LaNi_5$ composites by mechanically milling. The kinetics of the composites are superior to those of pure La_2Mg_{17} due to the composite consisting of a complex porous agglomeration of three phases: Mg_2Ni (~1 μm), La (~100 nm), and Mg. The absorption and desorption kinetics of Mg are catalytically enhanced by the intimate contact with Mg_2Ni, and to a lesser extent by the La phase.

Figure 4. (**a**) Hydriding kinetic curves for melted MmM_5 alloy and nano-phase composite of compositions MmM_5–10% Mg and MmM_5–30% Mg measured under isobaric conditions at 333 K (Reprinted with permission from [43]. Copyright 2002 Elsevier); (**b**) SEM micrograph of MmM_5–10% Mg powder mixture milled for 20 h (Reprinted with permission from [44]. Copyright 2003 Springer).

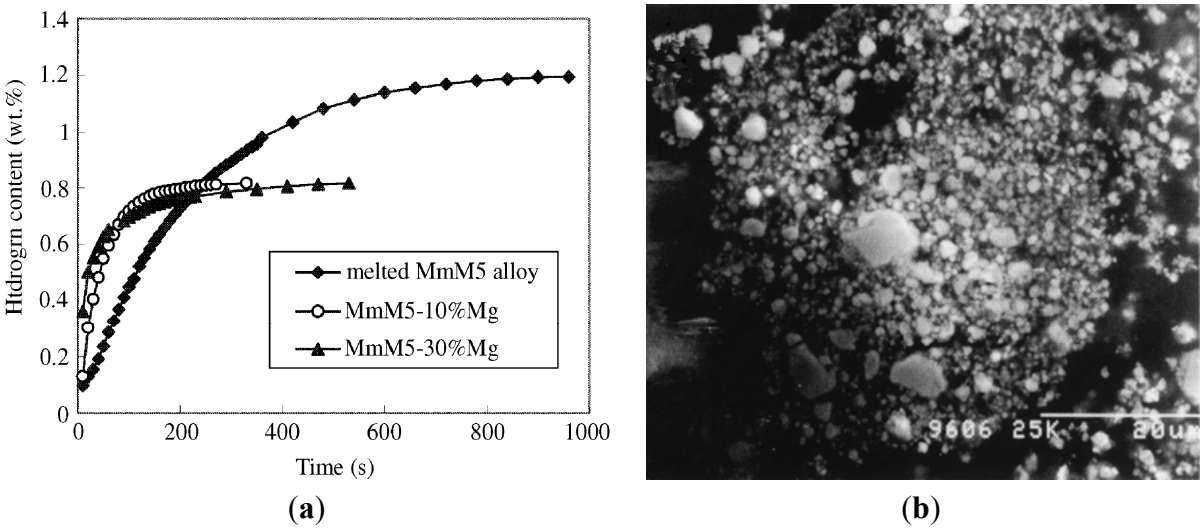

(**a**) (**b**)

4. Strategies for Tuning the Thermodynamics of Mg-Based Alloys

As described above, the hydrogen absorption/desorption kinetics have been improved substantially for Mg-based alloys. However, the high thermodynamic stability of MgH_2 is still a big hurdle for lowering the hydrogen desorption temperature of Mg-based hydrides. Effective attempts, such as alloying, nanostructuring, and changing the hydriding/dehydriding reaction route, have been made to tune the thermodynamics of Mg-based alloys.

4.1. Alloying

Mg forms the stable hydride MgH_2 with negative enthalpy ($\Delta H = -75$ kJ/mol). If Mg alloys are made with a hydride non-forming element, the hydriding reaction enthalpy can be decreased. Therefore, alloying is a traditional and effective strategy for altering the thermodynamics of Mg-based alloys.

One of the typical examples is Mg_2Ni (Ni is the hydride non-forming element), which can react with H_2 to form Mg_2NiH_4. The formation enthalpy of Mg_2NiH_4 (−64.5 kJ/mol) is lower than that of MgH_2 [18]. Morinaga *et al.* [46] found that hydrogen interacted more strongly with Ni atoms rather than Mg atoms in Mg_2NiH_4. This Ni–H interaction in Mg_2NiH_4 is much weaker than the Mg–H interaction in pure MgH_2, and leads to a lower formation enthalpy of Mg_2NiH_4. However, Mg_2NiH_4 has a lower hydrogen storage capacity than MgH_2. Similar to the Mg–Ni system, Mg and Cu can form

the Mg_2Cu alloy. During hydrogenation, Mg_2Cu decomposes to MgH_2 and $MgCu_2$ [47], and the equilibrium temperature for 1 bar hydrogen pressure is reduced to about 240 °C. Unfortunately, this reaction is irreversible.

Mg and Fe are immiscible, but a ternary hydride Mg_2FeH_6 can be formed in the presence of hydrogen [48]. Mg_2FeH_6 is very attractive as a hydrogen storage material because of its high volumetric and gravimetric hydrogen capacity, up to 150 kg/m^3 and 5.5 wt %, respectively. However, the formation enthalpy of Mg_2FeH_6 (−77.4 kJ/mol [49]) is higher than that of MgH_2. In addition, preparation of Mg_2FeH_6 is difficult as Mg and Fe do not form any intermetallic compounds. Mg and Co can react with H_2 under certain conditions to form Mg_2CoH_5. The gravimetric and volume density of Mg_2CoH_5 are 4.5 wt % and 100 kg/m^3, respectively. However, the dissociation heat of Mg_2CoH_5 is 86 kJ/mol [50], and Mg_2CoH_5 is not easy to synthesize because Mg_2Co does not exist. Ti also does not form an alloy with Mg under conventional conditions. Kyoi *et al.* [51] prepared a Mg_7TiH_x hydride by reacting MgH_2 with $TiH_{1.9}$ at 8 GPa and 873 K in a high-pressure anvil cell. Mg_7TiH_x decomposes into Mg and $TiH_{1.9}$ with the release of 4.7 wt % hydrogen, and the desorption temperature is around 605 K, which is 130 K lower than that of MgH_2.

Cd is the only element that can form a complete mutual solid solution with Mg under equilibrium conditions. Skripnyuk *et al.* [52] prepared the Mg_3Cd alloy by ball milling. As shown in Figure 5, no measurable pressure hysteresis was observed from the PCI, and there is a short horizontal section in the pressure plateau between 0.1 wt % and 0.3 wt % of H_2 corresponding to pure Mg. The subsequent pressure plateau was sloped and the formation enthalpies of the hydride calculated by the van't Hoff equation were 76.3 ± 1, 65.2 ± 1, 65.2 ± 2, and 65.5 ± 3 kJ/mol for the alloys containing 0.25, 1.55, 1.85, and 2.00 wt % hydrogen, respectively.

Based on the above results, alloying Mg with some elements can tune the thermodynamics of MgH_2. However, some limits cannot be ignored: the hydrogen capacity decreases sharply after alloying, and the reaction is often irreversible because of the bonds between Mg and the other element breaking during the process of hydrogenation.

Figure 5. Pressure-composition-temperature curves of the Mg_3Cd alloy in the temperature range 250–300 °C [52] (Reprinted with permission by T. Nejat Veziroglu, the founding editor-in-chief of IJHE).

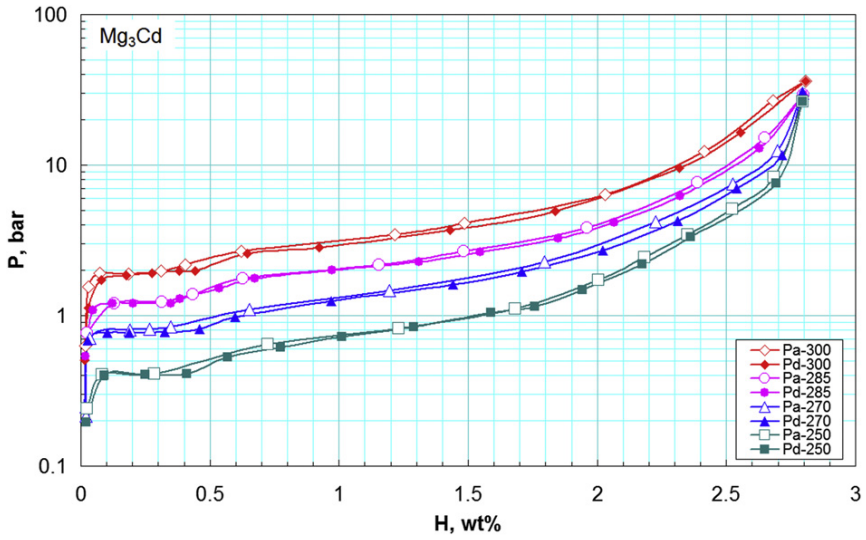

4.2. Nanostructuring

Nanostructuring can not only enhance the kinetics of Mg-based alloys, as mentioned in the previous section, it can also destabilize the thermodynamics of MgH_2. Wagemans *et al.* [53] investigated MgH_2 using quantum mechanical calculations and found that nanosized MgH_2 clusters have much lower desorption enthalpy (63 kJ/mol) than bulk MgH_2, enabling hydrogen desorption at lower temperatures from nanoclusters than from the bulk. The desorption temperature of MgH_2 clusters (size of ~0.9 nm) is only 200 °C.

The surface energy contributes significantly to the overall energy for the nanoparticles. Taking into account the surface energy, the total energy change upon dehydrogenation of the metal hydride will depend on the particle radius *r*, and can be expressed as [54,55]

$$\Delta G = \Delta G_0 + RT \ln \frac{p}{p_0} + \frac{3V_M \Delta_{M \to MH2}(\gamma, r)}{r} \quad (1)$$

with the volume-adjusted surface energy difference $\Delta_{M \to MH2}$ given by [55]

$$3V_M \Delta_{M \to MH2}(\gamma, r) = \left[\gamma_{MH2}(r) \left(\frac{V_{MH2}}{V_m} \right)^{\frac{2}{3}} - \gamma_M(r) \right] + E_{ads} \quad (2)$$

Because the surface energies might change during hydrogenation, the extra term E_{ads} is included. γ_{MH2} and γ_M are the surface energies of the hydride and metal. If $\gamma_{MH2} > \gamma_M$, decreasing the size of the nanoparticles will lower the stability of the hydride. Based on Equations (1) and (2), the formation enthalpy of sphere MgH_2 with radii smaller than 5 nm will decrease 20% compared with that of bulk MgH_2 in the same size. The high-density grain boundary in nanocrystalline Mg-based hydrides has a similar effect. Ouyang *et al.* [56] prepared the $Mg_{2.9}Ni$ film with a preferential orientated nanocrystalline structure via magnetron sputtering. The PCI curves of the $Mg_{2.9}Ni$ film are shown in Figure 6, and the lowest desorption temperature of this film was 497 K, which is much lower than that for bulk Mg with conventional grain size. This is because the interfacial energy of nanocrystalline Mg/Mg_2Ni is greatly increased, which can decrease the energy barrier for the formation of new phases. They used a simplified model to estimate the extra energy stored in the interface. By including the extra stored free energy, the formation enthalpies of Mg_2NiH_4 and MgH_2 decreased to −59.5 and −69.5 kJ/mol, respectively, and the reaction temperatures of Mg_2NiH_4 and MgH_2 decreased to 487.7 and 514.8 K, respectively, and are close to their experimental values. In addition, hydrogen first desorbs from Mg_2NiH_4, and then hydrogen desorption from MgH_2 becomes easier because of the stress caused by neighboring Mg_2Ni decomposed from Mg_2NiH_4.

Lu *et al.* [57] prepared a nanostructured MgH_2–$0.1TiH_2$ material by ultrahigh-energy-high-pressure ball milling. The grain size of the powder after milling was 5–10 nm with a uniform distribution of TiH_2 among the MgH_2 particles. Both the nanosize and the addition of TiH_2 contributed to the improvement of the kinetics and thermodynamics. The ΔH value for the dehydrogenation of MgH_2–$0.1TiH_2$ was 68 kJ/mol, which is lower than that of bulk MgH_2.

Chen *et al.* [58] produced Mg nanowires by a vapor-transport method using commercial Mg powder. The diameters of three Mg nanowires were 30–50 nm, 80–100 nm, and 150–170 nm. Both the

kinetics and thermodynamics of the Mg nanowires were better than those of bulk Mg/MgH_2. The activation energies of hydriding/dehydriding were 33.5/38.8, 38.7/46.5 and 70.3/81.1 kJ/mol, and the ΔH's for dehydriding of the hydride samples were 65.3, 65.9, and 67.2 kJ/mol. Moreover, as shown in Figure 7 [59], first-principles DFT calculations gave the dehydrogenation enthalpies for the MgH_2 bulk, nanowires, and single molecule as 74.0, 37.6, and −16.4 kJ/mol, respectively. These results indicate that decreasing the diameter leads to thermodynamic destabilization of MgH_2 nanowires, and that hydrogen desorption is possible at room temperature for MgH_2 nanowire of a diameter of 0.85 nm [59]. However, the nanowires could not maintain their structure after several hydrogenation/dehydrogenation cycles.

Figure 6. Pressure-composition isotherm curves of the $Mg_{2.9}Ni$ thin film measured at different temperatures: (**a**) 573 K; (**b**) 547 K; (**c**) 529 K; and (**d**) 497 K (Reprinted with permission from [56]. Copyright 2007 AIP Publishing LLC).

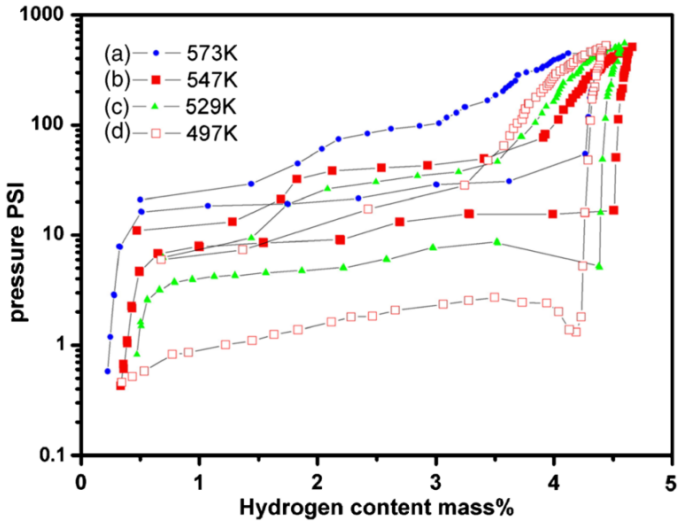

Figure 7. Significant difference of thermodynamic properties (**a**) and electronic structures among molecule (**b**); nanowire (**c**) and bulk (**d**) of Mg/MgH_2 (Reprinted with permission from [59]. Copyright 2009 Elsevier).

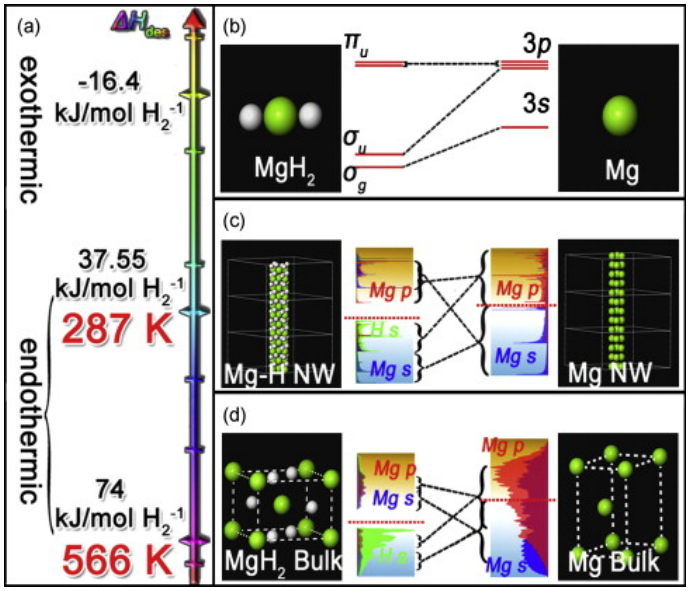

To stabilize the Mg/MgH_2 at the nano-scale, a recently developed strategy is to confine Mg/MgH_2 in a scaffold or matrix. Konarova *et al.* [60] synthesized MgH_2 particles by wet impregnation within the pores of the mesoporous materials SBA15 and CMK3. The thermal desorption behavior of MgH_2/CMK3 compounds were studied by varying the MgH_2 loading amount in CMK3. MgH_2/CMK3 compounds with 20 wt % loading released hydrogen at a temperature of 253 °C. Its corresponding decomposition enthalpy was 52.38 ± 2.16 kJ/mol. This means that there is a substantial destabilization of the thermodynamics of the Mg-MgH_2 reaction by nanoconfinement. Fichtner *et al.* [15] prepared MgH_2 nanoparticles with a size of less than 3 nm by hydrogenation of Bu_2Mg inside the pores of a carbon scaffold. Because the particles were small and the interaction between the particle and the support created strain in the nanoparticles, a significant decrease of the reaction enthalpy (63.8 ± 0.5 kJ/mol) and entropy (117.2 ± 0.8 J/mol) was obtained compared with the bulk materials. Although the reaction enthalpy greatly decreased, the decrease of the desorption temperature was only 11 °C because of the countereffect of the decreased reaction entropy. This result demonstrated that significant entropy change can occur, even though previous studies considered entropy to be a constant valve of about 130 J/(mol·K). Buckley *et al.* [16] used a mechanochemical method to synthesize MgH_2 nanoparticles embedded in a LiCl salt matrix. When the size of MgH_2 nanoparticles was ~7 nm, the decomposition reaction enthalpy decreased from ΔH_{bulk} = 74.06 ± 0.42 kJ/mol to ΔH_{nano} = 71.22 ± 0.49 kJ/mol. However, the reaction entropy also decreased from ΔS_{bulk} = 133.4 ± 0.7 J/(mol·K) to ΔS_{nano} = 129.6 ± 0.8 J/(mol·K). Thus, the desorption temperature of MgH_2 nanoparticles decreased from 281.8 ± 2.2 °C (bulk MgH_2) to 276.2 ± 2.4 °C, which is less than expected from the enthalpy change due to the decrease in ΔS.

In summary, nanostructuring can improve both the kinetics and thermodynamics of Mg-based hydrogen storage alloys. However, preparing materials with a sufficiently small dimension and maintaining the nanostructure during the cycles of hydrogenation/dehydrogenation is still difficult. In addition, size effects on a change in ΔS need to be further investigated.

4.3. Changing Reaction Pathway

Figure 8 shows that the hydride AH_2 can be destabilized by adding a reactive additive B. Without B, AH_2 decomposes into A and H_2 with a large enthalpy. In contrast, H_2 and stable AB_x form upon dehydrogenation after adding B, thus decreasing the reaction enthalpy, which raises the plateau pressure and decreases the dehydrogenation temperature [61].

A specific example of changing the reaction pathway to destabilize the thermodynamics of Mg/MgH_2 is to add Si to create the following reaction [62]:

$$MgH_2 + Si \rightarrow Mg_2Si + 2H_2 \quad (3)$$

The desorption enthalpy decreased to 36.4 kJ/mol due to the formation of Mg_2Si in Equation (3). However, this system suffers from poor reversibility and large capacity loss. Similarly, Walker *et al.* [63] milled MgH_2 with Ge under an Ar atmosphere (Equation (4)). The desorption temperature of MgH_2/Ge dramatically decreased to 130 °C. Unfortunately, the desorption product Mg_2Ge could not absorb hydrogen to form MgH_2 and Ge.

$$MgH_2 + Ge \rightarrow Mg_2Ge + 2H_2 \quad (4)$$

Obviously, the above two systems are irreversible. In addition, the additives Si and Ge cannot form hydrides, so the hydrogen capacity would be partially lost. However, using hydrides as additives can minimize this loss. Based on this, Vajo *et al.* [64] milled MgH_2 with $LiBH_4$. The dehydrogenation reaction can be expressed as

$$MgH_2 + 2LiBH_4 \leftrightarrow 2LiH + MgB_2 + 4H_2 \quad (5)$$

This reaction has a relatively small enthalpy of ΔH = 46 kJ/mol. Both MgH_2 and $LiBH_4$ are destabilized by the formation of MgB_2. However, MgB_2 is too stable to make the reaction reversible.

Al is also a reactive additive for MgH_2. The reaction occurs via two steps [65]:

$$2MgH_2 + 3Al \leftrightarrow Mg_2Al_3 + 2H_2 \quad (6)$$

$$9MgH_2 + 4Mg_2Al_3 \leftrightarrow Mg_{17}Al_{12} + 9H_2 \quad (7)$$

For the first step (Equation (6)), the reaction enthalpy is approximately 62.7 kJ/mol. Although the whole dehydriding reaction enthalpy is 77.7 kJ/mol, which is slightly higher than that of pure MgH_2, the whole reaction entropy increased from 139 to 144 J/(mol·K). Therefore, the desorption temperature of MgH_2-Al would be slightly lower than pure MgH_2 [66]. The system can reversibly store 4.4 wt % H_2.

By mechanical alloying, a reversible hydriding/dehydriding reaction for Mg(In) solid solution was developed by Zhong *et al.* [67]. At temperatures above 573 K, the path of the hydriding/dehydriding reaction for Mg(In) solid solution is as follows:

$$Mg(In) + H_2 \leftrightarrow MgH_2 + \beta \quad (8)$$

In the hydriding reaction, Mg(In) solid solution transforms to MgH_2 and MgIn (β phase), while in the dehydriding reaction, MgH_2 and MgIn can fully transform back to Mg(In). The enthalpy of this reaction is obviously less than pure Mg, and the plateau pressure of dehydriding is significantly higher. The decrease of the desorption enthalpy is related to the In content in the Mg(In) solid solution, and the enthalpy decreases from 78 kJ/mol for pure Mg to 68 kJ/mol for $Mg_{95}In_5$ with a hydrogen storage capacity of greater than 5 wt %.

Figure 8. Generalized enthalpy diagram illustrating destabilization by alloy formation upon dehydrogenation (Reprinted with permission from [61]. Copyright 2007 Elsevier).

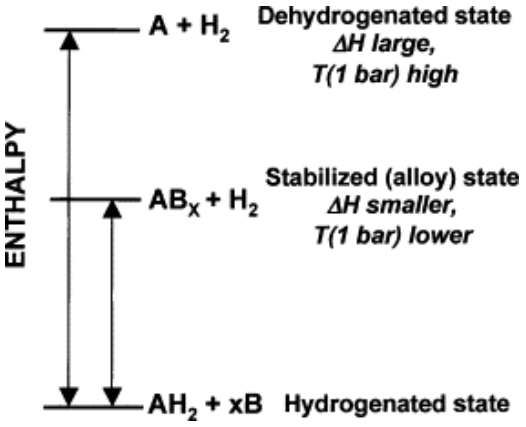

Destabilizing the thermodynamics of Mg-based alloys by changing the reaction pathway has the common disadvantage that the reaction is not completely reversible. Nevertheless, it provides a new route to tune the thermodynamics of Mg/MgH_2. It is worth noting that Mg(In) solid solution is completely reversible after dehydrogenation and the thermodynamic hydrogen sorption properties are altered. However, In is too expensive to be used on a large scale and the decrease of the enthalpy is not sufficient to make it cost efficient. Future research should focus on replacing In with cheaper elements, to further decrease the enthalpy and increase the kinetics.

4.4. Other Methods

Compared with bulk and powder materials, thin films often exhibit different properties. Higuchi *et al.* [68] investigated the hydrogen storage properties of nanocomposite three-layered Pd(50 nm)/Mg(x nm)/Pd(50 nm) films. With increasing thickness of the Mg film (x), the temperature corresponding to the maximum dehydrogenation rate decreased from 192 °C at x = 25 nm to 87 °C at x = 800 nm. This improvement can be explained by the cooperative phenomenon due to the elastic interaction between nanostructured Mg and Pd layers. The Pd/Mg/Pd film with a thick Mg layer would peel off from the substrate upon hydrogen uptake. For dehydrogenation, hydrogen in the up and down Pd films desorbs first, then the compression stress is induced on the up and down surfaces of the middle Mg film. As a result, hydrogen in the Mg film becomes unstable and leads to low temperature dehydrogenation. While Pd/Mg/Pd with a thin Mg layer does not peel off from the substrate upon hydrogenation, and Mg exhibits a martensite-like transformation, resulting in only a small compression stress on the Mg film plane leading to the weak cooperative interaction.

To improve the hydrogenation properties of Mg, Wang and Ouyang et al. prepared Mg–Ni thin films, and Mg/MmM_x and $Mg\text{-}Ni/MmM_5$ multi-layer films [69–74]. They prepared the Mg/MmM_5 multi-layer film via magnetron sputtering, and X-ray diffraction (XRD) analysis showed that most of the Mg was hydrogenated and dehydrogenated at about 523 K, which is about 100 K lower than the dehydrogenation temperature of pure Mg film. The microstructure of the multi-layer film was investigated in detail (Figure 9) [69,70]. The MmM_5 layer is composed of two regions: one is an amorphous region approximately 4 nm thick at the bottom of the layer, and the other is a nanocrystalline region on top of the amorphous region. The Mg layer is also composed of two regions: a randomly orientated nanocrystalline region 50 nm thick at the bottom of the layer, and a columnar crystallite region on top of the nanocrystalline region. Most of the columnar crystallites have their (001) directions parallel to the growth direction. All of the interfaces between different layers are clean without interface phases. The hydrogenation properties of Mg can be improved when the MmM_5 layer is inserted between the nanocrystalline Mg layers. A remarkable decrease of the hydrogenation/dehydrogenation temperature was achieved in the Mg/Mm–Ni multi-layer film prepared by evaporation deposition. Mg can be fully hydrogenated at 423 K and the hydrogen desorbs at 473 K. The decrease in hydrogenation/dehydrogenation temperature can be attributed to the catalytic roles of the $Nd(La)Ni_3$ and Mg_2Ni phases [72].

Baldi *et al.* [75] reported that the thermodynamics of hydrogen absorption in Mg can be tailored through elastic constraints. The equilibrium pressures of Mg films covered with Ni or Pd are much higher than those of Mg films capped with Ti, Nb, or V. Because Ti, Nb, and V are immiscible with

Mg, the Mg layer is free to expand upon hydrogen uptake. However, Ni and Pd are Mg-alloy-forming elements, and there is strong bonding between Mg and Ni or Pd. Therefore, elastic clamping exists at the interface, leading to the occurrence of hydrogenation under high plateau pressure. The effect of the clamping is greater the thinner the Mg layer, and the plateau pressure increases with decreasing Mg thickness. A 10-nm-thick Mg film has an equilibrium pressure more than 200 times higher than bulk Mg. Thus, elastic clamping offers an alternative route for tuning the thermodynamics of Mg–H.

Figure 9. HRTEM and TEM images of the cross-sections of the (**a**) MmM_5 layer and (**b**) Mg layer in the Mg/MmM_5 multi-layer film [69,70]. (Reprinted with permission from [69]. Copyright 2004 John Wiley and Sons. And reprinted with permission by T. Nejat Veziroglu, the founding editor-in-chief of IJHE.)

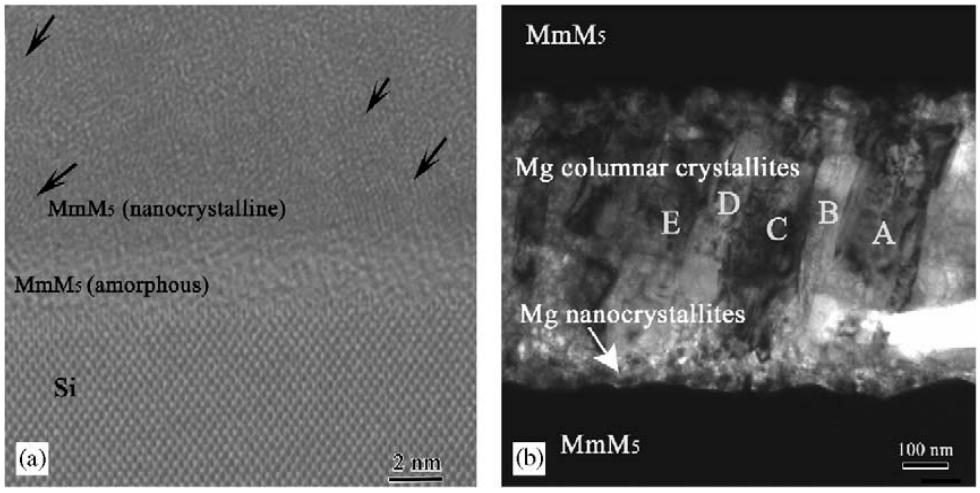

However, Chung *et al.* [76] showed that strain is not responsible for the increase in the equilibrium pressure for Mg thin films capped with a Pd layer, because MgH_2 was formed with near zero stress. It was the Mg–Pd alloy formed in the intermixed region at the Mg/Pd interface that increased the equilibrium pressure. The intermixing layer between the Mg and Pd layers was clearly observed by TEM and HRTEM, while the interface between Ti and Mg shows no intermixed region. The hydrogenation reaction of Mg-Pd is different from pure Mg, and can be represented by

$$\left(\frac{1}{1-x}\right)Mg_{1-x}Pd_x + H_2 \leftrightarrow MgH_2 + \left(\frac{x}{1-x}\right)Pd \quad (9)$$

The net enthalpy for the above reaction is −56 kJ/mol [77], which is smaller than that of pure Mg hydrogenation and, therefore, the equilibrium hydrogen pressure is higher. Ye *et al.* [78] prepared Mg/Pd multi-layer films by magnetron sputtering and also observed that the same dense Mg–Pd alloy Mg_6Pd formed along the interface between Mg and Pd, and even inside the Mg layers after the films were activated at 473 K for 2 h (Figure 10). The films could absorb and desorb about 2.5 wt % hydrogen at a low temperature of 323 K. The low hydrogenation/dehydrogenation temperature can be attributed to the extra interfacial free energy in the thin films and the catalytic effect of Pd.

The ΔH values for some improved Mg-based alloys mentioned above are listed in Table 3, which illustrate that alloying, nanostructuring, and changing the reaction pathway are effective ways to alter the thermodynamics of Mg/MgH_2.

Table 3. ΔH for improved Mg-based alloys in some works.

Strategies	Mg-based alloys	ΔH (kJ/mol)
Alloying	Mg_2NiH_4 [18]	64.5
	Mg_3Cd–H [52]	65.2
Nanostructuring	nanostructured MgH_2–0.1TiH_2 [57]	68
	Mg nanowires (30–50 nm) [58]	65.3
	MgH_2/CMK3 compounds [60]	52.38 ± 2.16
	MgH_2/ACF composite [15]	63.8 ± 0.5
Changing the reaction pathway	MgH_2/Si system [62]	36.4
	MgH_2/$LiBH_4$ system [64]	46
	Mg(In)–H system [67]	68

Figure 10. Bright-field TEM image of Mg/Pd multi-layer film activated at 473 K for 2 h under hydrogen pressure of 30 bar (Reprinted with permission from [78]. Copyright 2010 Elsevier).

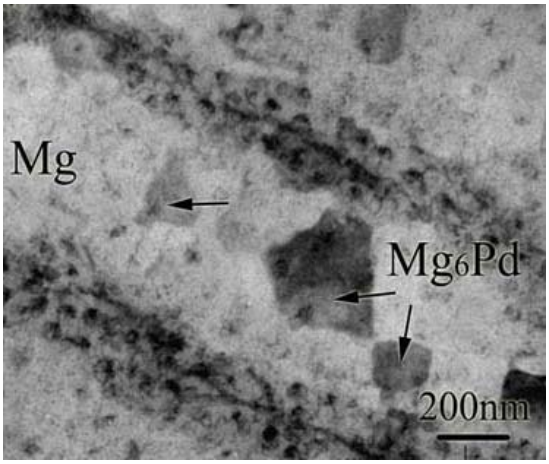

5. Summary and Prospects

Hydrogen storage materials and technology are the key issues in the realization of a hydrogen economy. Mg-based alloys show great promise because of their relatively high hydrogen storage capacity and abundance. Substantial progress has been made in improving the hydrogen absorption/desorption kinetics of Mg-based alloys. However, the thermodynamics of MgH_2 are still a big challenge for the practical application of Mg-based hydrogen storage alloys.

Alloying, nanostructuring, and changing the reaction pathway can effectively destabilize MgH_2. However, other problems arise, such as the loss of hydrogen storage capacity, the poor stability of the nanostructure, and the irreversibility of the reaction. The hydrogen capacity of MgH_2 is close to the value of the ultimate DOE target (7.5 wt %), leaving little room to improve the thermodynamics by alloying [79]. Mixing Mg-based alloys with a compound that is itself a hydride is a possibility. Moreover, it is difficult to prepare Mg-based nanostructures with controlled size, and it is therefore necessary to develop new strategies to produce ideal nano-Mg/MgH_2. It is worth noting that the Mg(In) solid solution can be reversibly formed by dehydriding its hydrogenated products, and has a lower reaction enthalpy than pure Mg. However, Mg(In) has poor kinetics. Finding a reversible system

with a high hydrogen capacity and excellent kinetics, and then effectively tailoring the reaction enthalpy of the system, would be a solution to solve the thermodynamic tuning of Mg-based hydrogen storage alloys. There are still many challenges in this field and much work needs to be done to realize the hydrogen economy of the future.

Acknowledgments

This work was financially supported by the Ministry of Science and Technology of China (No. 2010CB631302), the National Natural Science Foundation of China (Nos. U1201241 and 51271078), and KLGHEI (KLB11003).

Conflicts of Interest

The authors declare no conflict of interest.

References and Notes

1. Schlapbach, L.; Züttel, A. Hydrogen-storage materials for mobile applications. *Nature* **2001**, *414*, 353–358.
2. Sandí, G. Hydrogen storage and its limitations. *Electrochem. Soc. Interface* **2004**, *13*, 40–44.
3. Züttel, A. Hydrogen storage methods. *Naturwissenschaften* **2004**, *91*, 157–172.
4. Züttel, A. Materials for hydrogen storage. *Mater. Today* **2003**, *6*, 24–33.
5. van Vucht, J.H.N.; Kuijpers, F.A.; Bruning, H.C.A.M. Reversible room-temperature absorption of large quantities of hydrogen by intermetallic compounds. *Philips Res. Rep.* **1970**, *25*, 133–140.
6. Iwakura, C.; Fukuda, K.; Senoh, H.; Inoue, H.; Matsuoka, M.; Yamamoto, Y. Electrochemical characterization of $MmNi_{4.0-x}Mn_{0.75}Al_{0.25}Co_x$ electrodes as a function of cobalt content. *Electrochim. Acta* **1998**, *43*, 2041–2046.
7. Zhao, X.; Ma, L. Recent progress in hydrogen storage alloys for nickel/metal hydride secondary batteries. *Int. J. Hydrog. Energy* **2009**, *34*, 4788–4796.
8. Bououdina, M.; Grant, D.; Walker, G. Review on hydrogen absorbing materials—structure, microstructure, and thermodynamic properties. *Int. J. Hydrog. Energy* **2006**, *31*, 177–182.
9. Chen, J.; Takeshita, H.T.; Tanaka, H.; Kuriyama, N.; Sakai, T.; Uehara, I.; Haruta, M. Hydriding properties of $LaNi_3$ and $CaNi_3$ and their substitutes with $PuNi_3$-type structure. *J. Alloy. Compd.* **2000**, *302*, 304–313.
10. Kohno, T.; Yoshida, H.; Kanda, M. Hydrogen storage properties of $La(Ni_{0.9}M_{0.1})_3$ alloys. *J. Alloy. Compd.* **2004**, *363*, 254–257.
11. Chen, J.; Kuriyama, N.; Takeshita, H.T.; Tanaka, H.; Sakai, T.; Haruta, M. Hydrogen storage alloys with $PuNi_3$-type structure as metal hydride electrodes. *Electrochem. Solid State Lett.* **2000**, *3*, 249–252.
12. Peng, C.H.; Zhu, M. Microstructure and hydrogen storage properties of a multi-phase $Ml_{0.7}Mg_{0.3}Ni_{3.2}$ hydrogen storage alloy. *J. Alloy. Compd.* **2004**, *375*, 324–329.

13. Zhu, M.; Peng, C.H.; Ouyang, L.Z.; Tong, Y.Q. The effect of nanocrystalline formation on the hydrogen storage properties of AB_3-base Ml–Mg–Ni multi-phase alloys. *J. Alloy. Compd.* **2006**, *426*, 316–321.
14. Stetson, N. *Hydrogen Storage Sub-Program Overview*; Technical Report for FY 2012 Annual Progress Report: Washington, WA, USA, December 2012; pp. IV:3–IV:10.
15. Zhao-Karger, Z.; Hu, J.; Roth, A.; Wang, D.; Kubel, C.; Lohstroh, W.; Fichtner, M. Altered thermodynamic and kinetic properties of MgH_2 infiltrated in microporous scaffold. *Chem. Commun.* **2010**, *46*, 8353–8355.
16. Paskevicius, M.; Sheppard, D.A.; Buckley, C.E. Thermodynamic changes in mechanochemically synthesized magnesium hydride nanoparticles. *J. Am. Chem. Soc.* **2010**, *132*, 5077–5083.
17. Stampfer, J.F.; Holley, C.E.; Suttle, J.F. The magnesium-hydrogen system 1–3. *J. Am. Chem. Soc.* **1960**, *82*, 3504–3508.
18. Reilly, J.J.; Wiswall, R.H. Reaction of hydrogen with alloys of magnesium and nickel and the formation of Mg_2NiH_4. *Inorg. Chem.* **1968**, *7*, 2254–2256.
19. Pedersen, A.S.; Kjøller, J.; Larsen, B.; Vigeholm, B. Magnesium for hydrogen storage. *Int. J. Hydrog. Energy* **1983**, *8*, 205–211.
20. Friedlmeier, G.M.; Bolcich, J.C. Production and characterization of Mg-10 wt % Ni alloys for hydrogen storage. *Int. J. Hydrog. Energy* **1988**, *13*, 467–474.
21. Shao, H.; Wang, Y.; Xu, H.; Li, X. Hydrogen storage properties of magnesium ultrafine particles prepared by hydrogen plasma-metal reaction. *Mater. Sci. Eng.* **2004**, *110*, 221–226.
22. Bardhan, R.; Ruminski, A.M.; Brand, A.; Urban, J.J. Magnesium nanocrystal-polymer composites: A new platform for designer hydrogen storage materials. *Energy Environ. Sci.* **2011**, *4*, 4882–4895.
23. Zaluska, A.; Zaluski, L.; Ström-Olsen, J.O. Nanocrystalline magnesium for hydrogen storage. *J. Alloy. Compd.* **1999**, *288*, 217–225.
24. Huot, J.; Liang, G.; Boily, S.; Van Neste, A.; Schulz, R. Structural study and hydrogen sorption kinetics of ball-milled magnesium hydride. *J. Alloy. Compd.* **1999**, *293–295*, 495–500.
25. Aguey-Zinsou, K.-F.; Ares-Fernandez, J.-R. Hydrogen in magnesium: New perspectives toward functional stores. *Energy Environ. Sci.* **2010**, *3*, 526–543.
26. Vajeeston, P.; Ravindran, P.; Hauback, B.C.; Fjellvåg, H.; Kjekshus, A.; Furuseth, S.; Hanfland, M. Structural stability and pressure-induced phase transitions in MgH_2. *Phys. Rev.* **2006**, *73*, 224102:1–224102:8.
27. Tanniru, M.; Tien, H.Y.; Ebrahimi, F. Study of the dehydrogenation behavior of magnesium hydride. *Scripta Mater.* **2010**, *63*, 58–60.
28. Martin, M.; Gommel, C.; Borkhart, C.; Fromm, E. Absorption and desorption kinetics of hydrogen storage alloys. *J. Alloy. Compd.* **1996**, *238*, 193–201.
29. Liang, G.; Huot, J.; Boily, S.; Van Neste, A.; Schulz, R. Catalytic effect of transition metals on hydrogen sorption in nanocrystalline ball milled MgH_2–Tm (Tm = Ti, V, Mn, Fe and Ni) systems. *J. Alloy. Compd.* **1999**, *292*, 247–252.
30. Oelerich, W.; Klassen, T.; Bormann, R. Metal oxides as catalysts for improved hydrogen sorption in nanocrystalline Mg-based materials. *J. Alloy. Compd.* **2001**, *315*, 237–242.

31. Barkhordarian, G.; Klassen, T.; Bormann, R. Fast hydrogen sorption kinetics of nanocrystalline mg using Nb_2O_5 as catalyst. *Scripta Mater.* **2003**, *49*, 213–217.
32. Barkhordarian, G.; Klassen, T.; Bormann, R. Catalytic mechanism of transition-metal compounds on Mg hydrogen sorption reaction. *J. Phys. Chem.* **2006**, *110*, 11020–11024.
33. Jeon, K.-J.; Moon, H.R.; Ruminski, A.M.; Jiang, B.; Kisielowski, C.; Bardhan, R.; Urban, J.J. Air-stable magnesium nanocomposites provide rapid and high-capacity hydrogen storage without using heavy-metal catalysts. *Nat. Mater.* **2011**, *10*, 286–290.
34. Ouyang, L.Z.; Qin, F.X.; Zhu, M. The hydrogen storage behavior of Mg_3La and $Mg_3LaNi_{0.1}$. *Scripta Mater.* **2006**, *55*, 1075–1078.
35. Ouyang, L.Z.; Yang, X.S.; Dong, H.W.; Zhu, M. Structure and hydrogen storage properties of Mg_3Pr and $Mg_3PrNi_{0.1}$ alloys. *Scripta Mater.* **2009**, *61*, 339–342.
36. Ouyang, L.Z.; Dong, H.W.; Peng, C.H.; Sun, L.X.; Zhu, M. A new type of Mg-based metal hydride with promising hydrogen storage properties. *Int. J. Hydrog. Energy* **2007**, *32*, 3929–3935.
37. Ouyang, L.Z.; Dong, H.W.; Zhu, M. Mg_3Mm compound based hydrogen storage materials. *J. Alloy. Compd.* **2007**, *446–447*, 124–128.
38. Ouyang, L.Z.; Yao, L.; Yang, X.S.; Li, L.Q.; Zhu, M. The effects of Co and Ni addition on the hydrogen storage properties of Mg_3Mm. *Int. J. Hydrog. Energy* **2010**, *35*, 8275–8280.
39. Liu, J.W.; Zou, C.C.; Wang, H.; Ouyang, L.Z.; Zhu, M. Facilitating de/hydrogenation by long-period stacking ordered structure in Mg based alloys. *Int. J. Hydrog. Energy* **2013**, *38*, 10438–10445.
40. Spassov, T.; Lyubenova, L.; Köster, U.; Baró, M.D. Mg–Ni–RE nanocrystalline alloys for hydrogen storage. *Mater. Sci. Eng.* **2004**, *375–377*, 794–799.
41. Spassov, T.; Köster, U. Hydrogenation of amorphous and nanocrystalline Mg-based alloys. *J. Alloy. Compd.* **1999**, *287*, 243–250.
42. Lin, H.J.; Ouyang, L.Z.; Wang, H.; Liu, J.W.; Zhu, M. Phase transition and hydrogen storage properties of melt-spun $Mg_3LaNi_{0.1}$ alloy. *Int. J. Hydrog. Energy* **2012**, *37*, 1145–1150.
43. Zhu, M.; Gao, Y.; Che, X.Z.; Yang, Y.Q.; Chung, C. Hydriding kinetics of nano-phase composite hydrogen storage alloys prepared by mechanical alloying of Mg and $MmNi_{5-x}(CoAlMn)_x$. *J. Alloy. Compd.* **2002**, *330–332*, 708–713.
44. Gao, Y.; Zeng, M.Q.; Li, B.L.; Zhu, M.; Chung, C.Y. Solid state reaction and formation of nano-phase composite hydrogen storage alloy by mechanical alloying of $MmNi_{3.5}(CoMnAl)_{1.5}$ and Mg. *J. Mater. Sci.* **2003**, *38*, 2499–2504.
45. Gross, K.J.; Chartouni, D.; Leroy, E.; Züttel, A.; Schlapbach, L. Mechanically milled Mg composites for hydrogen storage: The relationship between morphology and kinetics. *J. Alloy. Compd.* **1998**, *269*, 259–270.
46. Morinaga, M.; Yukawa, H. Nature of chemical bond and phase stability of hydrogen storage compounds. *Mater. Sci. Eng.* **2002**, *329–331*, 268–275.
47. Reilly, J.J.; Wiswall, R.H. Reaction of hydrogen with alloys of magnesium and copper. *Inorg. Chem.* **1967**, *6*, 2220–2223.
48. Porutsky, S.G.; Zhurakovsky, E.A.; Mogilevsky, S.A.; Verbetsky, V.N.; Bakuma, O.S.; Semenenko, K.N. Electronic structure of Mg_2FeH_6 and Mg_2CoH_5 hydrides and binding role of hydrogen in them. *Solid State Commun.* **1990**, *74*, 551–553.

49. Bogdanović, B.; Reiser, A.; Schlichte, K.; Spliethoff, B.; Tesche, B. Thermodynamics and dynamics of the Mg–Fe–H system and its potential for thermochemical thermal energy storage. *J. Alloy. Compd.* **2002**, *345*, 77–89.
50. Zolliker, P.; Yvon, K.; Fischer, P.; Schefer, J. Dimagnesium cobalt (I) pentahydride, Mg_2CoH_5, containing square-pyramidal pentahydrocobaltate(4-) CoH_5^{4-} anions. *Inorg. Chem.* **1985**, *24*, 4177–4180.
51. Kyoi, D.; Sato, T.; Rönnebro, E.; Kitamura, N.; Ueda, A.; Ito, M.; Katsuyama, S.; Hara, S.; Noréus, D.; Sakai, T. A new ternary magnesium–titanium hydride Mg_7TiH_x with hydrogen desorption properties better than both binary magnesium and titanium hydrides. *J. Alloy. Compd.* **2004**, *372*, 213–217.
52. Skripnyuk, V.M.; Rabkin, E. Mg_3Cd: A model alloy for studying the destabilization of magnesium hydride. *Int. J. Hydrog. Energy* **2012**, *37*, 10724–10732.
53. Wagemans, R.W.P.; van Lenthe, J.H.; de Jongh, P.E.; van Dillen, A.J.; de Jong, K.P. Hydrogen storage in magnesium clusters: Quantum chemical study. *J. Am. Chem. Soc.* **2005**, *127*, 16675–16680.
54. Bérubé, V.; Radtke, G.; Dresselhaus, M.S.; Chen, G. Size effects on the hydrogen storage properties of nanostructured metal hydrides: A review. *Int. J. Energy Res.* **2007**, *31*, 637–663.
55. Bérubé, V.; Chen, G.; Dresselhaus, M.S. Impact of nanostructuring on the enthalpy of formation of metal hydrides. *Int. J. Hydrog. Energy* **2008**, *33*, 4122–4131.
56. Ouyang, L.Z.; Ye, S.Y.; Dong, H.W.; Zhu, M. Effect of interfacial free energy on hydriding reaction of Mg-Ni thin films. *Appl. Phys. Lett.* **2007**, *90*, 021917:1–021917:3.
57. Lu, J.; Choi, Y.J.; Fang, Z.Z.; Sohn, H.Y.; Ronnebro, E. Hydrogen storage properties of nanosized $MgH_{2-0.1}$ TiH_2 prepared by ultrahigh-energy-high-pressure milling. *J. Am. Chem. Soc.* **2009**, *131*, 15843–15852.
58. Li, W.; Li, C.; Ma, H.; Chen, J. Magnesium nanowires: Enhanced kinetics for hydrogen absorption and desorption. *J. Am. Chem. Soc.* **2007**, *129*, 6710–6711.
59. Peng, B.; Li, L.; Ji, W.; Cheng, F.; Chen, J. A quantum chemical study on magnesium(Mg)/magnesium–hydrogen(Mg–H) nanowires. *J. Alloy. Compd.* **2009**, *484*, 308–313.
60. Konarova, M.; Tanksale, A.; Norberto Beltramini, J.; Lu, G.Q. Effects of nano-confinement on the hydrogen desorption properties of MgH_2. *Nano Energy* **2013**, *2*, 98–104.
61. Vajo, J.J.; Salguero, T.T.; Gross, A.F.; Skeith, S.L.; Olson, G.L. Thermodynamic destabilization and reaction kinetics in light metal hydride systems. *J. Alloy. Compd.* **2007**, *446–447*, 409–414.
62. Vajo, J.J.; Mertens, F.; Ahn, C.C.; Bowman, R.C.; Fultz, B. Altering hydrogen storage properties by hydride destabilization through alloy formation: LiH and MgH_2 destabilized with Si. *J. Phys. Chem.* **2004**, *108*, 13977–13983.
63. Walker, G.S.; Abbas, M.; Grant, D.M.; Udeh, C. Destabilisation of magnesium hydride by germanium as a new potential multicomponent hydrogen storage system. *Chem. Commun.* **2011**, *47*, 8001–8003.
64. Pinkerton, F.E.; Meyer, M.S.; Meisner, G.P.; Balogh, M.P.; Vajo, J.J. Phase boundaries and reversibility of $LiBH_4/MgH_2$ hydrogen storage material. *J. Phys. Chem.* **2007**, *111*, 12881–12885.

65. Bouaricha, S.; Dodelet, J.P.; Guay, D.; Huot, J.; Boily, S.; Schulz, R. Hydriding behavior of Mg–Al and leached Mg–Al compounds prepared by high-energy ball-milling. *J. Alloy. Compd.* **2000**, *297*, 282–293.
66. Andreasen, A. Hydrogenation properties of Mg–Al alloys. *Int. J. Hydrog. Energy* **2008**, *33*, 7489–7497.
67. Zhong, H.C.; Wang, H.; Liu, J.W.; Sun, D.L.; Zhu, M. Altered desorption enthalpy of MgH_2 by the reversible formation of Mg(In) solid solution. *Scripta Mater.* **2011**, *65*, 285–287.
68. Higuchi, K.; Yamamoto, K.; Kajioka, H.; Toiyama, K.; Honda, M.; Orimo, S.; Fujii, H. Remarkable hydrogen storage properties in three-layered Pd/Mg/Pd thin films. *J. Alloy. Compd.* **2002**, *330–332*, 526–530.
69. Ouyang, L.Z.; Wang, H.; Zhu, M.; Zou, J.; Chung, C.Y. Microstructure of MmM_5/Mg multi-layer hydrogen storage films prepared by magnetron sputtering. *Microsc. Res. Tech.* **2004**, *64*, 323–329.
70. Zhu, M.; Wang, H.; Ouyang, L.Z.; Zeng, M.Q. Composite structure and hydrogen storage properties in Mg-base alloys. *Int. J. Hydrog. Energy* **2006**, *31*, 251–257.
71. Wang, H.; Ouyang, L.Z.; Zeng, M.Q.; Zhu, M. Hydrogen storage properties of Mg and Mg-Ni films prepared by thermal evaporation. *Acta Metall Sin.* **2004**, *40*, 531–536.
72. Wang, H.; Ouyang, L.Z.; Zeng, M.Q.; Zhu, M. Hydrogen sorption properties of Mg/Mm–Ni multi-layer film prepared by thermal evaporation. *J. Alloy. Compd.* **2004**, *375*, 313–317.
73. Wang, H.; Ouyang, L.Z.; Peng, C.H.; Zeng, M.Q.; Chung, C.Y.; Zhu, M. MmM_5/Mg multi-layer hydrogen storage thin films prepared by dc magnetron sputtering. *J. Alloy. Compd.* **2004**, *370*, L4-L6.
74. Wang, H.; Ouyang, L.; Zeng, M.; Zhu, M. Microstructure and hydrogen sorption properties of Mg–Ni/MmM_5 multi-layer film by magnetron sputtering. *Int. J. Hydrog. Energy* **2004**, *29*, 1389–1392.
75. Baldi, A.; Gonzalez-Silveira, M.; Palmisano, V.; Dam, B.; Griessen, R. Destabilization of the Mg–H system through elastic constraints. *Phys. Rev. Lett.* **2009**, *102*, 226102:1–226102:4.
76. Chung, C.J.; Lee, S.-C.; Groves, J.R.; Brower, E.N.; Sinclair, R.; Clemens, B.M. Interfacial alloy hydride destabilization in Mg/Pd thin films. *Phys. Rev. Lett.* **2012**, *108*, 106102:1–106102:4.
77. Takeichi, N.; Tanaka, K.; Tanaka, H.; Kuriyama, N.; Ueda, T.T.; Tsukahara, M.; Miyamura, H.; Kikuchi, S. Hydrogen storage properties, metallographic structures and phase transitions of Mg-based alloys prepared by super lamination technique. *MRS Proc.* **2008**, *1128*, 1128-U01–1128-U04.
78. Ye, S.Y.; Chan, S.L.I.; Ouyang, L.Z.; Zhu, M. Hydrogen storage and structure variation in Mg/Pd multi-layer film. *J. Alloy. Compd.* **2010**, *504*, 493–497.
79. Cheng, F.Y.; Tao, Z.L.; Liang, J.; Chen, J. Efficient hydrogen storage with the combination of lightweight Mg/MgH_2 and nanostructures. *Chem. Commun.* **2012**, *48*, 7334–7343.